

Keyphrase Extraction with Dynamic Graph Convolutional Networks and Diversified Inference

Haoyu Zhang^{1*}, Dingkun Long^{2*}, Guangwei Xu², Pengjun Xie², Fei Huang², Ji Wang^{1†}

¹State Key Laboratory of High Performance Computing, National University of Defense Technology

²Alibaba Group

{zhanghaoyu10, wj}@nudt.edu.cn, {dingkun.ldk, kunka.xgw, chengchen.xpj, f.huang}@alibaba-inc.com

Abstract

Keyphrase extraction (KE) aims to summarize a set of phrases that accurately express a concept or a topic covered in a given document. Recently, Sequence-to-Sequence (*Seq2Seq*) based generative framework is widely used in KE task, and it has obtained competitive performance on various benchmarks. The main challenges of *Seq2Seq* methods lie in acquiring informative latent document representation and better modeling the compositionality of the target keyphrases set, which will directly affect the quality of generated keyphrases. In this paper, we propose to adopt the Dynamic Graph Convolutional Networks (DGCN) to solve the above two problems simultaneously. Concretely, we explore to integrate dependency trees with GCN for latent representation learning. Moreover, the graph structure in our model is dynamically modified during the learning process according to the generated keyphrases. To this end, our approach is able to explicitly learn the relations within the keyphrases collection and guarantee the information interchange between encoder and decoder in both directions. Extensive experiments on various KE benchmark datasets demonstrate the effectiveness of our approach.

1 Introduction

A keyphrase is a multi-word text representing highly abstractive information in a long document Hasan and Ng (2014). Keyphrase extraction (KE) is a task that aims to generate an appropriate keyphrase set for the given document, thus helping to identify salient contents and concepts from the document. Recently, the KE task has attracted much research interest since it serves as an important component of many downstream applications such as text summarization Liu et al. (2009), document classification Hulth and Megyesi (2006), information retrieval Kim et al. (2013) and question generation Subramanian et al. (2017).

Early KE systems commonly operate in an extractive manner Mihalcea and Tarau (2004); Medelyan, Frank, and Witten (2009), which usually consists of two steps: 1) selecting candidates from the source document using heuristic rules, and 2) ranking the candidates list to determine which is correct. However, the two-step ranking approaches are usually based on feature engineering, which is

labor-intensive. Motivated by the progress in sequence-to-sequence applications of neural networks, KE research’s focus has gradually shifted to deep learning methods. Meng et al. (2017) first formulate KE as a sequence generation problem and introduce an attentive Seq2Seq framework to generate the keyphrase sequence conditioned on the input document. Compared with traditional methods, the Seq2Seq based method achieves superior performance.

Seq2Seq based KE is exposed to two major challenges: 1) Document-level representation learning. For any Seq2Seq generative framework, the latent hidden representation is a very important factor, and its quality will directly affect the decoder’s performance. In KE task, the input is commonly a long document instead of a sentence, which poses a greater challenge to latent representation learning. 2) Modeling the compositionality of keyphrases set. The elements in the keyphrase set are dependent and correlated. That is, better modeling the inherent composition embodied in the keyphrase set during the learning process will effectively boost the diversity and quality of final results.

Recently, various approaches have been proposed to optimize the Seq2Seq generation framework in KE task. To learn a better latent representation, previous studies try to introduce different encoding structures (e.g., BiLSTM Meng et al. (2017), Graph Convolutional Networks Sun et al. (2019b) or using title guided encoder Chen et al. (2019). Another line of work tries to learn the composition of keyphrase set by generating the concatenation of all target keyphrases Yuan et al. (2018) or using coverage attention to reduce word repetition Zhao and Zhang (2019). Existing approaches for KE mainly focus on one of the certain challenges as discussed. However, the two factors mentioned above are correlated.

The observations mentioned above motivate us to study a more general approach to the Seq2Seq based KE task. In this work, we propose to use a dynamic graph convolutional network (DGCN) to address the two issues above simultaneously. We explore to incorporate the dependency tree for document representation learning in the encoder part. The syntactic dependency tree can help to locate key information in a document. In practice, the document graph G is constructed depending on the syntactic dependency tree, and then a convolution process will be operated over G .

On the other hand, we rethink the implication of com-

* Indicates equal contribution.

† Corresponding author.

positionality in the keyphrase set. In the training process of generative models, whether a candidate keyphrase should be generated not only hinges on the document itself, but also depends on the keyphrases that have already been generated. Therefore, a dynamic graph updating mechanism is introduced to explicitly modeling the inter-dependency among keyphrases. In our method, the graph structure in the encoder part will be dynamically updated according to the keyphrases generated in the decoder part. Concretely, after one keyphrase is decoded, its information will be transferred to modify the edge weights in the document graph through a score function, and the latent hidden representation will also be updated. In this approach, we could dynamically ensure the information exchange between encoder and decoder parts in both directions.

The contribution of this work is three-fold: 1) A novel generative framework, Div-DGCN, is proposed that leverages both the dynamic syntactic graph encoder and diversified inference process for KE. 2) A dynamic computation mechanism is adopted to model the compositionality in keyphrase set explicitly and then enhancing the information interchange between the encoder and decoder parts in the Seq2Seq architecture. 3) Extensive experiments conducted on five benchmarks show that our proposed method is effective against competitive baselines on several metrics.

2 Related Work

Keyphrase extraction problem is usually carried out via extractive or generative methods. Conventional extractive methods usually use the two-step strategy that first extracts the candidate phrases using rules (hand-crafted or syntactic pattern matching) and then ranks them based on supervised or unsupervised methods Mihalcea and Tarau (2004); Medelyan, Frank, and Witten (2009). Gollapalli, Li, and Yang (2017) used sequence labeling models to extract keyphrases from the document.

Our model is based on Seq2Seq generative architecture. In this line of work, CopyRNN Meng et al. (2017) is the first to cooperate copy mechanism to generate keyphrases. Since then, Seq2Seq based generative models have gradually become the mainstream in the KE task. Chen et al. (2019) proposed a title-guided Seq2Seq network to enhance the latent document representation. Zhao and Zhang (2019) introduced linguistic annotations for representation learning. Deep graph-based methods have been used for text representation learning in many NLP tasks such as text summarization Yasunaga et al. (2017), semantic role labeling Marcheggiani and Titov (2017a) and machine translation Bastings et al. (2017). In KE task, Sun et al. (2019b) proposed to leverage graph-based encoder to model document-level word salience globally. Compared to previous works, our model explores the syntactic structure and lets the global decoder side information flow to impact the encoder representation, thus generates more global-aware document latent representations. The idea to model dynamic node embedding was also studied in other tasks Pareja et al. (2019), however, these methods evolve the model parameters instead of the graph structure, thus is different from ours.

There are also many studies focusing on the diversity of generated keywords. The catSeqD is an extension of catSeq with orthogonal regularization Bousmalis et al. (2016) and target encoding. Chen et al. (2018) further proposed a review mechanism to model the correlation between the keyphrases explicitly. Lately, Chan et al. (2019) proposed a reinforcement learning based fine-tuning method, which fine-tunes the pre-trained models with adaptive rewards for generating more sufficient and accurate keyphrases. Chen et al. (2020) designed a soft/hard exclusion mechanism to enhance the diversity. The idea of enhancing diversity is roughly selecting results that have not been generated or ensuring the whole results covering the main semantic contents.

3 Problem Definition

Keyphrases are usually divided into two categories: *present* and *absent*, determined by whether the phrase appears in the source document Meng et al. (2017); Chan et al. (2019). In this work, we concentrate on present keyphrase generation problem (keyphrase extraction), which can be formulated as follows: given source document $\mathcal{D} = \{x_1, x_2, \dots, x_l\}$ with l words, the ground-truth keyphrase set is $\mathcal{Y} = \{y_1, y_2, \dots, y_n\}$ with n keyphrases. We split the keyphrase set into present keyphrases \mathcal{Y}^p and absent keyphrases \mathcal{Y}^a . The target of present keyphrase generation is \mathcal{Y}^p , and we denote \mathcal{Y}^p as \mathcal{Y} in the rest of this paper for brevity. Therefore, each keyphrase y_j in \mathcal{Y} is sequence of words: $y_j = \{x_{m_1}^j, x_{m_2}^j, \dots, x_{m_j}^j\}$. Since we formulate the problem as a sequence generation problem, all present keyphrases are concatenated by a special token ‘‘SEP’’ to compose the target sequence with another token ‘‘EOS’’ in the end: $\{y_1, \text{SEP}, y_2, \text{SEP}, \dots, \text{EOS}\}$.

4 Method

Based on the Seq2Seq framework, the overall architecture of the proposed Div-DGCN framework is depicted in Figure 1. It mainly consists of a syntactic GCN encoder, a GRU based decoder, and a dynamic computation mechanism that bidirectionally associates the encoder and decoder.

4.1 Syntactic GCN Encoder

As analyzed in Meng et al. (2020), keyword extraction model based on Seq2Seq architecture tends to generate repetitive candidate sequences, many of which are parent-child strings, and which will obviously hurt the diversity of generated results. To address this problem, we introduce syntactic information to help the encoder better locate semantically completed candidate phrases in sentences (more details can be found in the Appendix).

The syntactic GCN encoder aims at encoding a variable-length document \mathcal{D} into a latent representations $H = \{h_1, h_2, \dots, h_l\}, h_j \in \mathbb{R}^{d_h}$, where d_h is the latent vector dimension. We first map each word x_i in the source document into word embedding $e_i^w \in \mathbb{R}^{d_w}$, POS embedding $e_i^{pos} \in \mathbb{R}^{d_{pos}}$ (using its POS annotation) and position embedding Vaswani et al. (2017) $e_i^p \in \mathbb{R}^{d_p}$. The final word representation e_i is the concatenation of the three parts $[e_i^w; e_i^{pos}; e_i^p]$, d_w, d_{pos} and d_p represent the embedding size

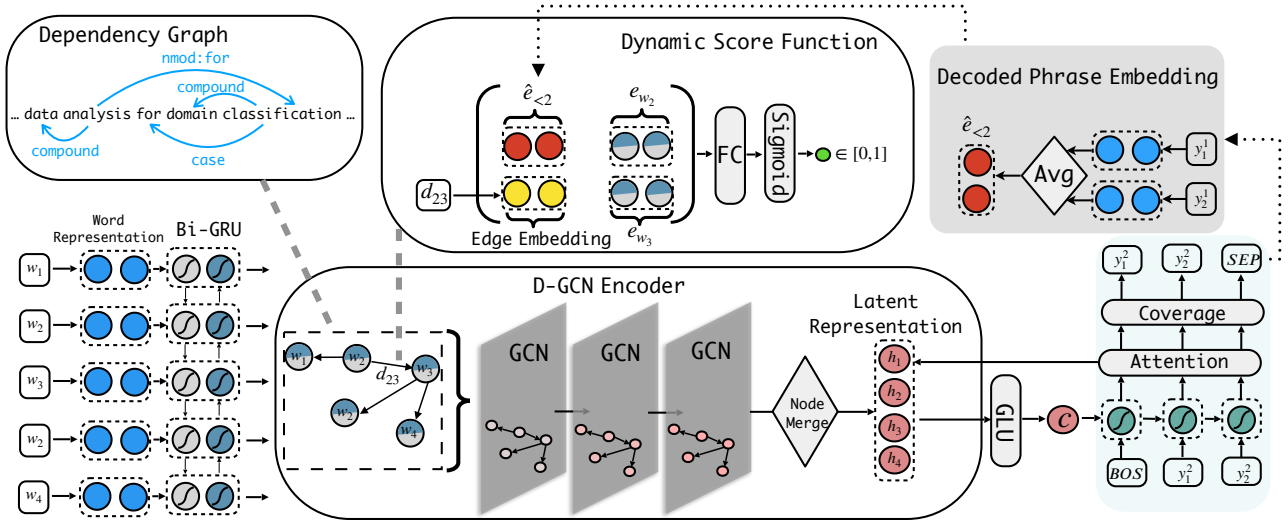


Figure 1: An overall architecture of our proposed Div-DGCN model. In this example, $\mathcal{D} = \{w_1, w_2, w_3, w_2, w_4\}$ and the first keyphrase $\{y_1^1, y_2^1\}$ has been generated.

of each part respectively. Before the GCN module, we apply a bidirectional GRU Chung et al. (2014) (BiGRU) to access the context features. Using the word sequence representation as input, the BiGRU network generates context-aware hidden states in both forward and backward directions. We can concatenate the corresponding representations in two directions as the output representations $H^0 = \{h_1^0, h_2^0, \dots, h_l^0\}$. **Syntactic Graph Construction** Given a source document \mathcal{D} with l words, we first split the document into sentences and get the sentence level syntactic dependency tree using Stanford Dependency Parser Qi et al. (2020). The dependency trees can be interpreted as word-level directed graph, where each node represents one word in the source document, and each edge represents a syntactic dependency path between two words. Mathematically, the directed graph G of the entire document can be represented as a sparse adjacency matrix $A \in \mathbb{R}^{l \times l}$. Previous works using syntactic trees and graph convolutional networks usually treated matrix A as a binary value matrix Marcheggiani and Titov (2017b); Sun et al. (2019a). Namely, $A_{ij} = 1$ if there exists a dependency path from word i to j or from word j to i , and otherwise $A_{ij} = 0$. In this work, to fully leverage the dependency tree structure information to represent the association between words pair, we use continuous value to indicate the closeness of such association. In particular, these continuous values are calculated by a score function that incorporating both the word embeddings and the dependency type. For the edge between word i and word j with dependency type d_{ij} , the weight A_{ij} in matrix A is calculated by:

$$A_{ij} = \sigma(W_e([e_i; e_j; e_{d_{ij}}^t])) \quad (1)$$

where $e_{d_{ij}}^t \in \mathbb{R}^{d_t}$ is the dependency type embedding, W_e is a parameter matrix and σ represents the sigmoid function. All calculated weights will located between 0 and 1. If there is no dependency path between word i and j , $A_{ij} = 0$.

Graph Convolutional Networks After constructing the

syntactic graphs G , we employ a multi-layer Graph Convolutional Network (GCN) to get the document representation, as shown in Figure 1. The output of the BiGRU network H^0 will be used to initial node embeddings in G . In each layer, the GCN encoder will only consider each node's one-hop neighborhood, then aggregate the neighbors' information when updating its representation. The update process in the k -th layer GCN can be represented as:

$$h_i^k = \text{ReLU}\left(\sum_{j=1}^l \frac{1}{d_i} A_{ij} (W^k h_j^{k-1} + b^k)\right) \quad (2)$$

where h_i^k is the i -th node representation at the k -th layer, W^k, b^k are layer-specific trainable weight/bias parameters, d_i is a normalization constant denoting the degree of node i , and we use ReLU Nair and Hinton (2010) as the activation function. For a N -layer GCN, the node representations are $H^N = \{h_1^N, \dots, h_l^N\}$. In the rest of the paper, we denote H^N as H .

For the keyphrase generation task, we seek to acquire a continuous representation of the entire document. However, the dependency trees are in sentence-level. Thus, we add a node merge layer to enhance the information interchange between sentences. Specifically, words share the same stem word are aggregated into only one representation through an average pooling function. Thus, the new sequential representation is $H = \{h_1, \dots, h_{l'}\}$, where l' notes the sequential length after the merge operation.

The final document representation (or the entire context vector) c is computed by a residual Gated Linear Unit (GLU) layer He et al. (2016) and an averaging layer:

$$H = H + (W_k H \otimes \sigma(W_l H)) \quad (3)$$

$$c = \frac{1}{|l'|} \sum_{i=1}^{l'} H_i \quad (4)$$

where \otimes denotes element-wise multiplication, and c is used to initialize the decoder hidden state.

4.2 Copy Decoder

The body of the decoder is a GRU network. At time step t , the hidden state s_t in GRU is updated based on the embedding of previous decoded word $e_{y_{t-1}}^w$ and the hidden state at time step $t-1$: $s_t = f(s_{t-1}, e_{y_{t-1}}^w), s_0 = c$. To cope with the Out-of-Vocabulary (OOV) challenge, we adopt a Pointer Generator See, Liu, and Manning (2017) style copy mechanism. For each document \mathcal{D} , a dynamic vocabulary \mathcal{V}_d is calculated to cover all tokens in \mathcal{D} as well as the pre-built static vocabulary \mathcal{V} . By attending the hidden state s_t to the latent document representations H , the copy distribution over \mathcal{V}_d is calculated as the final predictive distribution. In addition, we observe that keyphrases are located in different parts of the source document. Therefore, we adopt a coverage mechanism Chen et al. (2018) to prevent the predictive distribution from locating on a small portion of \mathcal{D} .

We utilize the beam search to decode keyphrase sequences. Beam search stores the top- B highly scoring candidates at each time step, where B is known as the beam width. When decoding the p -th keyphrase at its t -th word, the set of B candidate sequences can be denoted as $Y_t^p = \{\mathbf{y}_{1,[t]}^p, \dots, \mathbf{y}_{B,[t]}^p\}, \mathbf{y}_{b,[t]}^p \in \mathbb{R}^t$, thus, all choices at t -th time step over the dynamic vocabulary are $\mathcal{Y}_t^p = Y_{t-1}^p \times \mathcal{V}_d$. To reduce the search space, we leverage a phrase-level beam search method. The phrase-level beam search decodes each keyphrase individually, and once a keyphrase is decoded, the candidate sequence with the highest score will be picked. In this way, the optimization objective is represented as:

$$Y_t^p = \arg \max_{\mathbf{y}_{1,[t]}^p, \dots, \mathbf{y}_{B,[t]}^p \in \mathcal{Y}_t^p} \sum_{b \in [B]} \Theta(\mathbf{y}_{b,[t]}^p) \quad (5)$$

which indicates that we aim to select B sequences with maximum scores from $B \cdot |\mathcal{V}_d|$ members in \mathcal{Y}_t^p . For the sequence score function $\Theta(\cdot)$, we use the negative log probability sum with length penalty.

Diversified Inference To enhance the semantic diversity of generated keyphrases. Motivated by previous works Li, Monroe, and Jurafsky (2016); Shi et al. (2018), we propose a diversified inference algorithm for the phrase-level beam search via adding two terms. First, we add a phrase-level dissimilarity penalty (DP) term $\text{DP}(\mathbf{y}_{b,[t]}^p, \mathbf{y}^{<p})$ to the score function Θ , where $\mathbf{y}^{<p}$ denotes the first decoded $p-1$ keyphrases. A key motivation behind the dissimilarity term is that the current keyphrase should be different from previous decoded ones. Hence, we use the uni-gram and bi-gram overlap ratio to measure the dissimilarity between two sequences. On the other hand, as the standard beam search selects sequence based on the accumulated log probability of each token, nodes with very high score might dominate the search process, which will degrade the candidate search space and generate similar keyphrases. Thus, we introduce a sibling penalty (SP) term $\text{SP}(y_{b,t}^p)$ whose value is the log-probability rank of the t -th candidate token in the candidate sequence over $|\mathcal{V}_d|$. By incorporating the sibling penalty, we can filter the low-score candidates that have high-score ancestors. To this end, the final sequence score function is:

$$\hat{\Theta}(\mathbf{y}_{b,[t]}^p, \mathbf{y}^{<p}) = \Theta(\cdot) + \lambda_1 \text{DP}(\cdot) - \lambda_2 \text{SP}(y_{b,t}^p) \quad (6)$$

Algorithm 1: Inference Procedure

Input:
- $\mathcal{D} = \{x_1, \dots, x_l\}; \mathbf{y}^{<p} = \{y^1, \dots, y^{p-1}\}$
- Model parameters: θ
Perform beam search for the p -th keyphrase using beam width B
 $H^p, c^p = \text{ENCODER}(\mathcal{D}, \mathbf{y}^{<p}; \theta)$
for $t = 1, \dots, T$ **do**
 $P(y_{b,t}^p) = \text{DECODER}(y_{b,<t}^p, H^p, c^p; \theta)$
 $\mathcal{Y}_t^p = \mathcal{Y}_{t-1}^p \times P(y_{b,t}^p)$
 $\hat{\Theta}(\mathbf{y}_{b,[t]}^p) \leftarrow \Theta(\mathbf{y}_{b,[t]}^p) + \lambda_1 \text{DP}(\mathbf{y}_{b,[t]}^p, \mathbf{y}^{<p}) - \lambda_2 \text{SP}(y_{b,t}^p)$
 $Y_t^p \leftarrow \arg \max_{\mathbf{y}_{1,[t]}^p, \dots, \mathbf{y}_{B,[t]}^p} \sum_{b \in [B]} \hat{\Theta}(\mathbf{y}_{b,[t]}^p)$
Return $y^p = \arg \max(Y_T^p)$ using $\hat{\Theta}(\cdot)$ as the predicted p -th keyphrase.

where λ_1 and λ_2 are hyper-parameters, which control the importance of each term. The diversified inference process of a single keyphrase is illustrated in Algorithm 1.

4.3 Dynamic Graph Convolutional Networks

The use of syntactic tree information and graph convolutional networks allows us to obtain a better document representation. However, to generate high-quality keyphrases, it is also important to model the inter-relationship between keyphrases. To address this issue, previous attempts mainly focus on modifying the decoder structure. The modification of decoder part means that the decoder process still depends on the static hidden representation c . In this work, we model the inter-relationship between keyphrases set in a global view. As discussed, the decoding process of p -th keyphrase depends both on the source document and the previously decoded keyphrases. This observation motivates us to transform the hidden representation to evolve together with the decoding process dynamically. Moreover, the score function design in graph G allows us to carry out this dynamic process at a very low cost.

Specifically, for the input graph G , we modify the edge weights in matrix A after decoding each keyphrase. The score function in Eq. 1 is extended to the following form:

$$A_{ij}^p = \sigma(W_e([e_i; e_j; e_{d_{ij}}^t; \hat{e}_{<p}])) \quad (7)$$

when decoding the p -th keyphrase, the decoded keyphrases word sequence is $y^{<p} = \{y_1^1, \dots, y_{l_1}^1, \dots, y_1^{p-1}, \dots, y_{l_{p-1}}^{p-1}\}$, and the decoded phrase embedding $\hat{e}_{<p}$ in Eq. 7 represents the average pooling results of all decoded word embeddings. When $p=1$, $\hat{e}_{<p}$ is a zero vector. That is, the relatedness between two words are not only determined by its word embedding and dependency types corresponds, but also depends on the previously decoded contents. Once a keyphrase is generated, we will update the adjacent matrix A of G through Eq. 7. In this way, the hidden representation c will also be updated. As a result, during the encoding process, the graph G is capable to dynamically extract information which is informative for the decoder part.

The dynamic computation mechanism enable us to transmit the information of decoder to the encoder, then informs

the ungenerated keyphrases of what have been already generated. Consequently, we explicitly model the relationship between each element in the keyphrases set.

4.4 Training

Given training data $\{\mathcal{D}, \mathcal{Y}\}$, \mathcal{D} notes the document and \mathcal{Y} represents the concatenated keyphrases. The loss function with parameters θ is the average negative log-likelihood on all ground-truth words in the keyphrase sequences:

$$\mathcal{L}(\theta) = - \sum_{p=1}^n \sum_{j=1}^{l_p} \log(P(y_j^p | y_{<j}^p, y^{<p}, \mathcal{D}; \theta)) \quad (8)$$

5 Experiment

We thoroughly evaluate the performance of our method on five benchmarks, and we use several competitive approaches as baselines. Also, several auxiliary experiments are conducted to analyze the effectiveness of our method. All experiments are repeated three times using different random seeds and the averaged results are reported.

5.1 Implementation Details

We utilize Stanford Parser Qi et al. (2020) for the dependency parsing and POS annotation. We use the Pre-trained 300 dimension FasText word embeddings Bojanowski et al. (2016) and keep the word embeddings learnable during training. Our model variants are trained using the Adam optimizer Kingma and Ba (2015) with a batch size 128 and an initial learning rate 0.001. During training, we use a dropout rate of 0.2 and a gradient clipping threshold of 0.2. We train the model for 20 epochs, and every 2000 iterations the validation perplexity (ppl) are evaluated. The learning rate is reduced by half if the validation ppl does not drop, three contiguous stagnant ppl will trigger the early stop of training. All characters in the document and keyphrase set are lower-cased and all digits are replaced with a special token.

Decoding Process We use exactly the same pre-process, post-process and performance evaluation processes with previous studies Yuan et al. (2018); Chan et al. (2019). Following Sun et al. (2019b), we set beam search with beam width 100 in the decoding module on all test sets. If the termination symbol '[EOS]' is encountered or the number of keyphrases generated exceeds the pre-defined maximum number, the decoding process will be terminated. To ensure the fairness of the comparison, the testing process is consistent with Sun et al. (2019b) and all repeated keyphrases in the generated sequences are removed before evaluation.

Hyper-parameters Table 5 in the Appendix shows all hyper-parameters used in our model variants. The values of these hyper-parameters are chosen empirically. In the beam search process, we choose the same length penalty factor with previous work Sun et al. (2019b). The two diversified factors λ_1 and λ_2 are chosen separately depending on the performance improvement on the validation set. The detailed performance curves are also included in the Appendix.

Datasets We conduct experiments on five scientific article datasets, including Kp20k Meng et al. (2017), Inspec Hulth (2003), Krapivin Krapivin, Autaeu, and Marchese (2009),

Dataset	#samples	#present	length
training data			
Kp20k	464,676	2.94	2.01
validation data			
Kp20k	20,000	3.49	1.86
test data			
Inspec	500	7.20	2.40
NUS	211	5.64	1.93
SemEval	100	6.12	2.07
Krapivin	400	3.24	1.86
Kp20k	20,000	3.31	1.86

Table 1: Statistics of five datasets.

NUS Nguyen and Kan (2007) and SemEval Kim et al. (2010). Each sample from these datasets consists of the title, abstract, and the target keyphrases. We concatenate the title and abstract to compose the input document. Following previous studies, we train our model on the Kp20k dataset. Then we evaluate our model on five benchmark test datasets. Table 1 illustrates more details of the datasets.

Baselines We compare our methods with state-of-the-art KE systems include: CatSeq / CatSeqD Yuan et al. (2018), CatSeqTG Chen et al. (2019), CatSeqD-2RF₁ / CatSeqTG-2RF₁ Chan et al. (2019), DivGraphPointer Sun et al. (2019b) and ExHiRD-h Chen et al. (2020). In fact, excluding the syntactic DGCN encoder and the diversified inference, our model is equal to CatSeqD except we only use copy probability.

Evaluation Metrics We use $F_1 @ M$ proposed in Yuan et al. (2018) and $F_1 @ 5$ as our evaluation metrics. $F_1 @ M$ calculates the F1 score by comparing all the generated keyphrases with ground-truth keyphrase. Namely, M is determined by the number of generated keyphrases. When calculating $F_1 @ 5$, if the model predicts less than 5 keyphrases, random wrong answers are appended for evaluation. Marco average is used to aggregate the evaluation scores for all samples. Note that we use Porter Stemmer for preprocessing to determine whether the two keyphrases are matching. These two metrics are **commonly used** in previous works including Chan et al. (2019); Chen et al. (2020). We also introduce a ranking-based metric, Normalized Discounted Cumulative Gain (NDCG) Wang et al. (2013) to evaluate our model performances. Finally, we add experimental results using another version of $F_1 @ 5$ and $F_1 @ 10$ adopted by Meng et al. (2019) as evaluation metrics and put it in the Appendix.

5.2 Overall Results

The final results are reported in Table 2, from which we can observe that: our Div-DGCN model shows competitive performances compared with previously proposed methods on all five datasets. Our model exceeds the SOTA method on $F_1 @ 5$ performances by a large margin (average **13.5%** performance gain on 5 test sets), which proves the diversity of our generated results. In terms of the $F_1 @ M$ metric, the performance of Div-DGCN is slightly inferior to the SOTA method, but there is still a significant improvement compared to the baseline model. Comparing with previous

Model	Inspec		Krapivin		NUS		SemEval		KP20k	
	$F_1@M$	$F_1@5$								
Transformer Vaswani et al. (2017)	0.254	0.210	0.328	0.252	-	-	0.310	0.257	0.360	0.282
catSeq Yuan et al. (2018)	0.262	0.225	0.354	0.269	0.397	0.323	0.283	0.242	0.367	0.291
catSeqD Yuan et al. (2018)	0.263	0.219	0.349	0.264	0.394	0.321	0.274	0.233	0.363	0.285
catSeqCorr Chen et al. (2018)	0.269	0.227	0.349	0.265	0.390	0.319	0.290	0.246	0.365	0.289
catSeqTG Chen et al. (2019)	0.270	0.229	0.366	0.282	0.393	0.325	0.290	0.246	0.366	0.292
catSeqD-2 RF_1 Chan et al. (2019)	0.292	0.242	0.360	0.282	0.419	0.353	0.316	0.272	0.379	0.305
ExHiRD-h Chen et al. (2020)	0.291	0.253	0.347	0.286	-	-	0.335	0.284	0.374	0.311
GCN	0.312	0.261	0.331	0.262	0.391	0.325	0.303	0.264	0.350	0.281
Div-GCN	0.360	0.331	0.324	0.280	0.389	0.371	0.317	0.289	0.343	0.304
DGCN	0.327	0.275	0.354	0.284	0.397	0.328	0.319	0.280	0.359	0.290
Div-DGCN	0.376	0.348	0.345	0.313	0.391	0.379	0.323	0.320	0.349	0.313
Normalized Discounted Cumulative Gain @10 (NDCG@10)										
DivGraphPointer Sun et al. (2019b)	0.503		0.591		0.518		0.534		0.532	
CatSeqTG-2 RF_1 Chan et al. (2019)	0.614		0.586		0.780		0.677		0.592	
GCN	0.657		0.582		0.787		0.677		0.590	
DGCN	0.663		0.597		0.797		0.704		0.616	
Div-DGCN	0.692		0.611		0.797		0.701		0.620	

Table 2: Results of present keyphrase prediction on five datasets. The best results are in bold. ‘‘GCN’’ denotes the model using syntactic GCN encoder. ‘‘DGCN’’ denotes the model using syntactic GCN encoder and dynamic computation mechanism. ‘‘Div-DGCN’’ and ‘‘Div-GCN’’ are the corresponding model variants decoding with diversified inference.

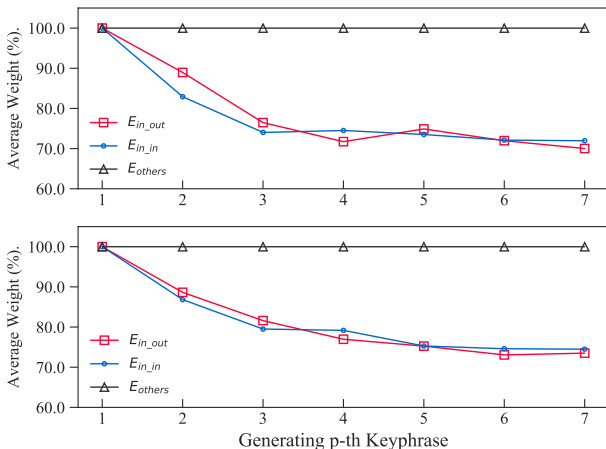


Figure 2: Average weight trends of particular edge types on Inspec (upper) and NUS (lower) test set.

works using $F_1@5$ and $F_1@10$ (see Appendix) as evaluation metrics, we observe that our Div-DGCN model presents a promising improvement against previous methods.

In the KE task, the Seq2Seq architecture tends to generate a larger number of candidates, but few of them (less than 5%) are unique Meng et al. (2020). These observations prove that the improvement on $F_1@5$ of Div-DGCN is due to the improvement of the model’s ability on generating accurate and diversify accurate keyphrases. On the other hand, our method focuses on generating keyphrases with higher diversity, but we also observe that the $F_1@M$ metric is in conflict with the the goal of diversity to some extent. Especially for datasets with relatively fewer ground-truth keyphrases, results with higher diversity will decrease

Datasets	# Nodes	# Edges	# E_{in_in}	# E_{in_out}
Inspec	145.27	374.07	40.64	75.82
Krapivin	197.24	532.32	19.66	72.48
NUS	240.81	627.68	34.97	109.00
SemEval	245.72	679.97	43.98	131.78

Table 3: The node and edge statistics on four test sets.

the $F_1@M$ value. Another line of work in KE task tends to uses $F_1@5$ and $F_1@10$ (without filling prediction) as evaluation metrics (see Appendix), $F_1@5$ is much higher than $F_1@10$ in most situations, which further proves that $F_1@M$ is somewhat cannot reflect the diversity of results.

Further, measured by ranking metric, comparing under the very similar decoding setting with Chan et al. (2019) and the exactly same decoding setting with Sun et al. (2019b), our model achieves an average of 5.5% improvements against them. This data also illustrates that our model can generate high-quality and diverse keyphrase lists.

Ablation Study We examine the performances of different model variants *based on the same decoding settings* to evaluate the impact of different modules. From the results in Table 2, we can see that: 1) For both GCN and Div-GCN setting, dynamic computation mechanism brings stable performance improvement on $F_1@M$ (2.5% and 6.9% on KP20K and Krapivin) and significant improvement on $F_1@5$, which proves the effectiveness of the dynamic computation mechanism. 2) On most test sets, the diversified inference lifts the $F_1@5$ by a large margin but degrades the $F_1@M$ performances. It might because the DI process tends to generate longer sequences, which will cause the value of $F_1@M$ lower in some cases. 3) According to the rank-based metric NDCG@10, the DGCN encoder is essential to

<p>Title: secure and efficient <u>key management</u> in <u>mobile ad hoc networks</u></p> <p>Abstract: in mobile ad hoc networks , due to unreliable wireless media , host mobility and lack of infrastructure , providing <u>secure communications</u> is a big challenge . usually , cryptographic techniques are used for secure communications in wired and wireless networks . symmetric and asymmetric cryptography have their advantages and disadvantages . in fact , any cryptographic means is ineffective if its <u>key management</u> is weak . key management is also a central aspect for <u>security</u> in mobile ad hoc networks . in <u>mobile ad hoc networks</u> , the computational load and complexity for key management are strongly subject to restriction by the node ‘s available resources and the dynamic nature of network topology . we propose a secure and efficient key management (sekm) framework for mobile ad hoc networks . sekm builds a <u>public key infrastructure</u> (<u>pki</u>) by applying a <u>secret sharing</u> scheme and using an underlying server groups . we give detailed information on the formation and maintenance of the server groups ... , an efficient <u>server group</u> updating scheme is proposed ...</p> <p>Oracle: mobile ad hoc networks ; key management ; secret sharing ; security ; server group</p> <p>CatSeqTG-2RF₁: <u>key management</u> ; <u>mobile ad hoc networks</u> ; <u>public key infrastructure</u> ; <u>pki</u></p> <p>ExHiRD-h: <u>key management</u> ; <u>mobile ad hoc networks</u> ; <u>secure communications</u> ; <u>public key infrastructure</u></p> <p>DGCN: <u>key management</u> ; <u>mobile ad hoc networks</u> ; <u>secret sharing</u></p> <p>Div-DGCN: <u>mobile ad hoc networks</u> ; <u>key management</u> ; <u>security</u> ; <u>secret sharing</u> ; <u>server group</u></p>
--

Figure 3: A prediction example of baselines and our model variants. The correct keyphrases are underlined.

the model and achieves the best performances on three test sets. This result again proves that the inter-relation between keyphrases is important to the KE task.

5.3 Discussion and Analysis

Dynamic Graph Properties To examine the effectiveness of the DGCN, we record some properties of the dynamic syntactic graphs during the inference process. From the statistics in Table 3, we find that the graphs are very sparse since roughly only 2.6% of the nodes-pairs have edges between them. Besides, we calculate the average weights of the following three special edge types when decoding the p -th ($p \in [1, 2, \dots, 7]$) keyphrase. For edge e_{ij} connected with node i and node j : 1) if both node i and node j are ground-truth target phrase words, we classify the edge as \mathbf{E}_{in_in} ; 2) if only one of the nodes lies in the ground-truth target phrase word set, this edge is called as \mathbf{E}_{in_out} ; 3) all the other edges is classified to \mathbf{E}_{others} . As Figure 2 shows, the average weights of \mathbf{E}_{in_in} and \mathbf{E}_{in_out} types drops as the decoding process continues, while the average weights \mathbf{E}_{others} keeps steady. As Table 3 shows, \mathbf{E}_{in_in} accounts for no more than 10.8% (On Inspec) of all the edges and \mathbf{E}_{in_out} accounts for no more than 20.3% (On Inspec). The statistics prove that the dynamic structure modifies the graph by reducing the edge weights of related nodes while keeping most of the edge weights unchanged.

Model	Inspec		SemEval	
	Avg. #	Corr. #	Avg. #	Corr. #
oracle	7.20	-	6.12	-
catSeqTG-2RF ₁	3.45	1.41	3.73	1.48
ExHiRD-h	4.00	N/A	3.65	N/A
catSeqD	3.33	1.25	3.47	1.28
GCN	3.53	1.55	3.77	1.45
DGCN	3.58	1.60	4.05	1.58
Div-DGCN	5.40	2.26	6.10	1.91

Table 4: The abilities of predicting diversified and high-quality keyphrase set on two datasets. Avg. # is the average number of generated keyphrases. Corr. # is the average number of correctly predicted keyphrases.

Unique Keyphrase Numbers To better examine the diversity of generated keyphrase sequences, we study the average number of unique keyphrases as well as the corrected predicted keyphrase number to compare the predictive quality with several KE models. Due to page limitation, we cannot list the results of KP20K in Table 4, the average predicted keyphrase number and correct number in KP20K of our method is 4.90 and 1.45, much higher than which reported in ExHiRD-h Chen et al. (2020) paper (3.97 and 0.81). As Table 4 shows, compared to other models including our ablation variants, the Div-DGCN model generates much more keyphrases, which mitigates the insufficient generation problem, also the numbers of correctly predicted keyphrase are improved significantly (similar or higher precision when predicting more phrases). Compared to our backbone model catSeqD, the DGCN model also generates longer and more diverse outputs. The results illustrate the importance of the introduced syntactic-aware encoder and dynamic structure.

Case Study We show a prediction case in Figure 3. From the case, we observe that compared to the two SOTA models, our model predicts a more accurate keyphrase list. Also, compared to the ablation variant, the predicted results with diversified inference cover more topics in the source document. These results show that our model captures the relation in the keyphrase set and achieves better results.

6 Conclusion

Modeling informative latent representations as well as capturing keyphrase dependencies is essential to Seq2Seq keyphrase extraction models. In this work we propose a Div-DGCN framework to address these two issues by enhancing the encoder with syntactic graph and modifying the graph edge information in the keyphrase decoding process. Further enhanced with a diversified inference process, the model can generate accurate and diverse outputs. Experimental results show that our model can surpass previous competitive models on various metrics and benchmark datasets, proving its effectiveness.

References

- Bastings, J.; Titov, I.; Aziz, W.; Marcheggiani, D.; and Sima'an, K. 2017. Graph Convolutional Encoders for Syntax-aware Neural Machine Translation. In *EMNLP*, 1957–1967. The Association for Computer Linguistics.
- Bojanowski, P.; Grave, E.; Joulin, A.; and Mikolov, T. 2016. Enriching Word Vectors with Subword Information. *CoRR* abs/1607.04606.
- Bousmalis, K.; Trigeorgis, G.; Silberman, N.; Krishnan, D.; and Erhan, D. 2016. Domain Separation Networks. In *NIPS*, 343–351.
- Chan, H. P.; Chen, W.; Wang, L.; and King, I. 2019. Neural Keyphrase Generation via Reinforcement Learning with Adaptive Rewards. In *ACL (1)*, 2163–2174. The Association for Computer Linguistics.
- Chen, J.; Zhang, X.; Wu, Y.; Yan, Z.; and Li, Z. 2018. Keyphrase Generation with Correlation Constraints. In *EMNLP*, 4057–4066. The Association for Computer Linguistics.
- Chen, W.; Chan, H. P.; Li, P.; and King, I. 2020. Exclusive Hierarchical Decoding for Deep Keyphrase Generation. *CoRR* abs/2004.08511.
- Chen, W.; Gao, Y.; Zhang, J.; King, I.; and Lyu, M. R. 2019. Title-Guided Encoding for Keyphrase Generation. In *AAAI*, 6268–6275. AAAI Press.
- Chung, J.; Gülçehre, Ç.; Cho, K.; and Bengio, Y. 2014. Empirical Evaluation of Gated Recurrent Neural Networks on Sequence Modeling. *CoRR* abs/1412.3555.
- Gollapalli, S. D.; Li, X.; and Yang, P. 2017. Incorporating Expert Knowledge into Keyphrase Extraction. In *AAAI*, 3180–3187. AAAI Press.
- Hasan, K. S.; and Ng, V. 2014. Automatic Keyphrase Extraction: A Survey of the State of the Art. In *ACL (1)*, 1262–1273. The Association for Computer Linguistics.
- He, K.; Zhang, X.; Ren, S.; and Sun, J. 2016. Deep Residual Learning for Image Recognition. In *CVPR*, 770–778. IEEE Computer Society.
- Hulth, A. 2003. Improved Automatic Keyword Extraction Given More Linguistic Knowledge. In *EMNLP*. The Association for Computer Linguistics.
- Hulth, A.; and Megyesi, B. 2006. A Study on Automatically Extracted Keywords in Text Categorization. In *ACL*. The Association for Computer Linguistics.
- Kim, S. N.; Medelyan, O.; Kan, M.; and Baldwin, T. 2010. SemEval-2010 Task 5 : Automatic Keyphrase Extraction from Scientific Articles. In *SemEval@ACL*, 21–26. The Association for Computer Linguistics.
- Kim, Y.; Kim, M.; Cattle, A.; Otmakhova, J.; Park, S.; and Shin, H. 2013. Applying Graph-based Keyword Extraction to Document Retrieval. In *IJCNLP*, 864–868. The Association for Computer Linguistics.
- Kingma, D. P.; and Ba, J. 2015. Adam: A Method for Stochastic Optimization. In *ICLR (Poster)*.
- Krapivin, M.; Autaeu, A.; and Marchese, M. 2009. Large dataset for keyphrases extraction. Technical report, University of Trento.
- Li, J.; Monroe, W.; and Jurafsky, D. 2016. A Simple, Fast Diverse Decoding Algorithm for Neural Generation. *CoRR* abs/1611.08562.
- Liu, F.; Pennell, D.; Liu, F.; and Liu, Y. 2009. Unsupervised Approaches for Automatic Keyword Extraction Using Meeting Transcripts. In *HLT-NAACL*, 620–628. The Association for Computational Linguistics.
- Marcheggiani, D.; and Titov, I. 2017a. Encoding Sentences with Graph Convolutional Networks for Semantic Role Labeling. In *EMNLP*, 1506–1515. The Association for Computer Linguistics.
- Marcheggiani, D.; and Titov, I. 2017b. Encoding Sentences with Graph Convolutional Networks for Semantic Role Labeling. In *EMNLP*, 1506–1515. The Association for Computer Linguistics.
- Medelyan, O.; Frank, E.; and Witten, I. H. 2009. Human-competitive tagging using automatic keyphrase extraction. In *EMNLP*, 1318–1327. The Association for Computer Linguistics.
- Meng, R.; Yuan, X.; Wang, T.; Brusilovsky, P.; Trischler, A.; and He, D. 2019. Does Order Matter? An Empirical Study on Generating Multiple Keyphrases as a Sequence. *CoRR* abs/1909.03590.
- Meng, R.; Yuan, X.; Wang, T.; Zhao, S.; Trischler, A.; and He, D. 2020. An Empirical Study on Neural Keyphrase Generation. *ArXiv* abs/2009.10229.
- Meng, R.; Zhao, S.; Han, S.; He, D.; Brusilovsky, P.; and Chi, Y. 2017. Deep Keyphrase Generation. In *ACL (1)*, 582–592. The Association for Computer Linguistics.
- Mihalcea, R.; and Tarau, P. 2004. TextRank: Bringing Order into Text. In *EMNLP*, 404–411. The Association for Computer Linguistics.
- Nair, V.; and Hinton, G. E. 2010. Rectified linear units improve restricted boltzmann machines. In *ICML*, 807–814.
- Nguyen, T. D.; and Kan, M. 2007. Keyphrase Extraction in Scientific Publications. In *ICADL*, volume 4822, 317–326. Springer.
- Pareja, A.; Domeniconi, G.; Chen, J.; Ma, T.; Suzumura, T.; Kanezashi, H.; Kaler, T.; and Leiserson, C. E. 2019. EvolveGCN: Evolving Graph Convolutional Networks for Dynamic Graphs. *CoRR* abs/1902.10191.
- Qi, P.; Zhang, Y.; Zhang, Y.; Bolton, J.; and Manning, C. D. 2020. Stanza: A Python Natural Language Processing Toolkit for Many Human Languages. *CoRR* abs/2003.07082.
- See, A.; Liu, P. J.; and Manning, C. D. 2017. Get To The Point: Summarization with Pointer-Generator Networks. In *ACL (1)*, 1073–1083. The Association for Computer Linguistics.

- Shi, Z.; Chen, X.; Qiu, X.; and Huang, X. 2018. Toward Diverse Text Generation with Inverse Reinforcement Learning. In *IJCAI*, 4361–4367. ijcai.org.
- Subramanian, S.; Wang, T.; Yuan, X.; and Trischler, A. 2017. Neural Models for Key Phrase Detection and Question Generation. *CoRR* abs/1706.04560.
- Sun, K.; Zhang, R.; Mensah, S.; Mao, Y.; and Liu, X. 2019a. Aspect-Level Sentiment Analysis Via Convolution over Dependency Tree. In *EMNLP/IJCNLP (1)*, 5678–5687. The Association for Computer Linguistics.
- Sun, Z.; Tang, J.; Du, P.; Deng, Z.; and Nie, J. 2019b. DivGraphPointer: A Graph Pointer Network for Extracting Diverse Keyphrases. In *SIGIR*, 755–764. ACM.
- Vaswani, A.; Shazeer, N.; Parmar, N.; Uszkoreit, J.; Jones, L.; Gomez, A. N.; Kaiser, L.; and Polosukhin, I. 2017. Attention is All you Need. In *NIPS*, 5998–6008.
- Wang, Y.; Wang, L.; Li, Y.; He, D.; and Liu, T. 2013. A Theoretical Analysis of NDCG Type Ranking Measures. In *COLT*, volume 30, 25–54. [JMLR.org](http://jmlr.org).
- Yasunaga, M.; Zhang, R.; Meelu, K.; Pareek, A.; Srinivasan, K.; and Radev, D. R. 2017. Graph-based Neural Multi-Document Summarization. In *CoNLL*, 452–462. The Association for Computer Linguistics.
- Yuan, X.; Wang, T.; Meng, R.; Thaker, K.; Brusilovsky, P.; He, D.; and Trischler, A. 2018. One Size Does Not Fit All: Generating and Evaluating Variable Number of Keyphrases. *CoRR* abs/1810.05241.
- Zhao, J.; and Zhang, Y. 2019. Incorporating Linguistic Constraints into Keyphrase Generation. In *ACL (1)*, 5224–5233. The Association for Computer Linguistics.

Appendix A

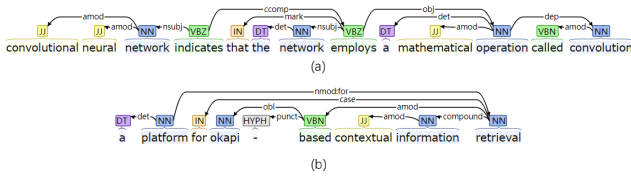


Figure 4: Syntactic dependency tree for two samples.

Why using the syntactic information

Syntactic tree helps to find possible candidate phrases in a sentence. As Figure 4-(a) shows, it captures "convolutional neural network" as a complete phrase rather than "neural network". Moreover, as Figure 4-(b) shows, the syntactic information provides a discontinuous phrase candidate "okapi based retrieval" based on long term dependencies.

Hyper-parameters

Hyper-parameters	Value
BiGRU Layer	1
Word Embedding Size (d_w)	300
Pos Embedding Size (d_{pos})	30
Position Embedding Size (d_p)	10
GCN (DGCN) layer	6
GCN Embedding Size (d_h)	400
Edge Embedding Size (d_e)	80
GRU Hidden Size	400
Decoder Layer	3
Phrase-Level Factor (λ_1)	1.0
Beam-Level Factor (λ_2)	0.1

Table 5: Hyper-parameters chosen for all models.

Data sources

We use the predictions released publicly¹ to calculate CatSeqTG-2RF₁'s NDCG@10 and average predicted/correct keyphrase numbers. We use the average predicted keyphrase numbers of ExHiRD-h as reported by its original paper.

Corpus and Evaluation

We use the public available pre-processed datasets². Also, we follow the previous work's evaluation process³.

The Diversified Inference Process

Due to the page limitation, we put the commented DI process here to show the procedure more clearly.

¹<https://github.com/kenchan0226/keyphrase-generation-rl>

²https://drive.google.com/file/d/1DbXV1mZXm_o9bgfwPV9PV0ZPcNo1cnLp/view

³https://github.com/kenchan0226/keyphrase-generation-rl/blob/master/evaluate_prediction.py

Algorithm 2: Inference Procedure

Input:

- $\mathcal{D} = \{x_1, \dots, x_l\}$; $\mathbf{y}^{<p} = \{y^1, \dots, y^{p-1}\}$

- Model parameters: θ

Perform beam search for the p -th keyphrase using beam width B

$H^p, c^p = \text{ENCODER}(D, \mathbf{y}^{<p}; \theta)$

for $t = 1, \dots, T$ do

```

// predictive probability for B
// groups over vocabulary  $\mathcal{Y}_d$ 
 $P(y_{b,t}^p) = \text{DECODER}(y_{b,<t}^p, H^p, c^p; \theta)$ 
//  $B \cdot |\mathcal{Y}_d|$  candidate sequences
 $\mathcal{Y}_t^p = \mathcal{Y}_{t-1}^p \times P(y_{b,t}^p)$ 
// calculate diversified sequence
// scores
 $\hat{\Theta}(\mathbf{y}_{b,[t]}^p) \leftarrow \Theta(\mathbf{y}_{b,[t]}^p) + \lambda_1 \text{DP}(\mathbf{y}_{b,[t]}^p; \mathbf{y}^{<p}) - \lambda_2 \text{SP}(y_{b,t}^p)$ 
// perform one step of beam search
 $Y_t^p \leftarrow \arg \max_{(\mathbf{y}_{1,[t]}^p, \dots, \mathbf{y}_{B,[t]}^p)} \sum_{b \in [B]} \hat{\Theta}(\mathbf{y}_{b,[t]}^p)$ 

```

Return $y^p = \arg \max(Y_T^p)$ using $\hat{\Theta}(\cdot)$ as the predicted p -th keyphrase.

Repeated Experiments

We conduct the experiment on each model variant for 3 times using different random seeds, and report the average performances in the paper for brevity. Table 7 lists the average and deviation values of each model on several metrics. The subscript represents the corresponding standard deviation value (e.g., 0.342_3 indicates 0.342 ± 0.003).

Impact of the Diversified Inference Factor

We search the two factors on Kp20k dev set separately, and use the combination of the two best factors. Our search space for the phrase-level factor λ_1 is $[0.1, 0.2, 0.5, 0.8, 1.0, 1.5, 2.0, 3.0, 5.0, 8.0, 10.0]$ and the search space for the beam-level factor λ_2 is $[0.01, 0.05, 0.1, 0.2, 0.5, 0.8, 1.0, 1.5, 2.0]$. The performance curves on KP20k dev set and several test sets are shown in Figure 5. We observe that λ_1 improves the $F_1@5$ by a large margin but degrades $F_1@M$, and λ_2 boosts the $F_1@M$ performances, so we choose these two metrics in Figure 5.

Comparison based on Other Metrics

In keyphrase extraction task, some studies choose to use the $F_1@M$ and filled version of $F_1@5$ as evaluation metrics (we choose these two metrics) while others evaluate the performances using $F_1@5$ and $F_1@10$. The latter $F_1@5$ does not fill random wrong predictions when prediction number is less than 5. To thoroughly evaluate the effectiveness of our model, we further compare the full model's performance on $F_1@5$ and $F_1@10$ in Table 6. Baseline methods listed in Table 6 only report these two metrics so we cannot compare to them in the experiments section of our paper. We find that our model exceeds the baselines by a relative large margin especially in $F_1@10$. Note that SKE-Large-Rank surpasses our method on several metrics but it uses the pretrained language model BERT-LARGE and thus takes the advantages on document representations.

Model	Inspec		Krapivin		NUS		SemEval		KP20k	
	$F_1@5$	$F_1@10$								
CopyRNN	0.278	0.342	0.311	0.266	0.334	0.326	0.293	0.304	0.333	0.262
CatSeqD(2018)	0.276	0.333	0.325	0.285	0.374	0.366	0.327	0.352	0.348	0.298
TG-Net(2019)	0.315	0.381	0.349	0.295	0.406	0.370	0.318	0.322	0.372	0.315
ParaNetT+CoAtt(2019)	0.296	0.357	0.329	0.282	0.360	0.350	0.311	0.312	0.360	0.289
SKE-Large-Rank(2020)	0.300	0.334	0.313	0.264	0.400	0.379	0.356	0.351	0.392	0.328
Div-DGCN	0.369	0.385	0.355	0.354	0.408	0.407	0.344	0.325	0.352	0.347

Table 6: Results of present keyphrase prediction based on other metrics. SKE-Large-Rank uses the pre-trained BERT large.

Model	Inspec		Krapivin		NUS		SemEval		KP20k	
	$F_1@M$	$F_1@5$	$F_1@M$	$F_1@5$	$F_1@M$	$F_1@5$	$F_1@M$	$F_1@5$	$F_1@M$	$F_1@5$
GCN	0.312 ₇	0.261 ₄	0.331 ₉	0.262 ₅	0.391 ₁₃	0.325 ₁₄	0.303 ₉	0.264 ₉	0.350 ₄	0.281 ₂
Div-GCN	0.360 ₈	0.331 ₆	0.324 ₅	0.280 ₃	0.389 ₇	0.371 ₁₁	0.317 ₆	0.289 ₄	0.343 ₁	0.304 ₂
DGCN	0.327 ₇	0.275 ₈	0.354 ₇	0.284 ₄	0.397 ₉	0.328 ₂	0.319 ₈	0.280 ₁₂	0.359 ₀	0.290 ₄
Div-DGCN	0.376₃	0.348₆	0.345 ₂	0.313₄	0.391 ₇	0.379₆	0.323 ₉	0.320₁₄	0.349 ₂	0.313₃
Normalized Discounted Cumulative Gain @10 (NDCG@10)										
GCN	0.657 ₅		0.582 ₂		0.787 ₉		0.677 ₁₅		0.590 ₆	
DGCN	0.663 ₃		0.597 ₃		0.797₇		0.704₁₀		0.616₅	
Div-DGCN	0.692₄		0.611₈		0.797₁₄		0.701 ₁₆		0.620₁	

Table 7: Results with standard deviation on all datasets.

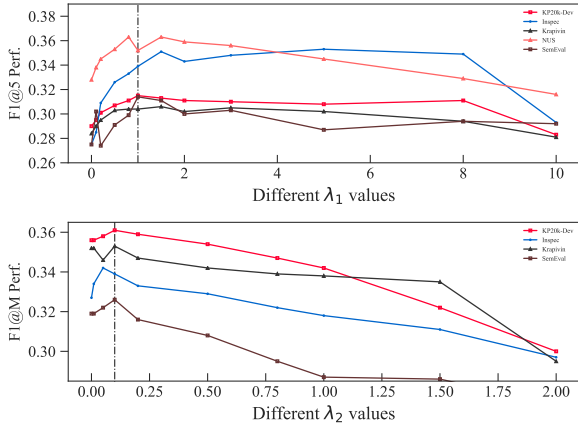


Figure 5: Performance curves of phrase-level factor λ_1 and beam-level factor λ_2 .